Evolution with Opponent-Learning Awareness

Yann Bouteiller Polytechnique Montreal Montreal, Canada Karthik Soma Polytechnique Montreal Montreal, Canada Giovanni Beltrame Polytechnique Montreal Montreal, Canada

ABSTRACT

The universe involves many independent co-learning agents as an ever-evolving part of our observed environment. Yet, in practice, Multi-Agent Reinforcement Learning (MARL) applications are usually constrained to small, homogeneous populations and remain computationally intensive. In this paper, we study how large heterogeneous populations of learning agents evolve in normalform games. We show how, under assumptions commonly made in the multi-armed bandit literature, Multi-Agent Policy Gradient closely resembles the Replicator Dynamic, and we further derive a fast, parallelizable implementation of Opponent-Learning Awareness tailored for evolutionary simulations. This enables us to simulate the evolution of very large populations made of heterogeneous co-learning agents, under both naive and advanced learning strategies. We demonstrate our approach in simulations of 200,000 agents, evolving in the classic games of Hawk-Dove, Stag-Hunt, and Rock-Paper-Scissors. Each game highlights distinct ways in which Opponent-Learning Awareness affects evolution.

KEYWORDS

Multi-agent reinforcement learning, Evolutionary game theory, Simulation, Opponent-learning awareness

ACM Reference Format:

Yann Bouteiller, Karthik Soma, and Giovanni Beltrame. 2024. Evolution with Opponent-Learning Awareness. *arXiv preprint*, 12 pages.

1 INTRODUCTION

While most Reinforcement Learning (RL) theory relies on the stationarity assumption [28], real-world situations are hardly ever truly stationary. Our universe is a place of perpetual change, where countless agents co-exist, co-learn and co-evolve. For any individual agent, other learning agents represent a fundamentally non-stationary part of the environment, and even more so when incentives are in conflict. In the realm of Reinforcement Learning, the study of this type of possibly adversarial non-stationarity [23] is a field known as Multi-Agent Reinforcement Learning (MARL).

While some notable achievements do tackle MARL scenarios, these are largely constrained by the high inherent complexity of multi-agent training. Successful MARL applications rarely feature more than a few agents, and in fact often resort to training a single neural network against one or few copies of itself. This powerful learning trick, named "self-play", was famously used to learn Go at a superhuman level [25], and competitive human-level team play in a video game [5]. On both occasions, the authors had to spend extreme amounts of compute, even though the number of agents involved was small and despite the computational savings

enabled by training a single replicated model (as opposed to independent agents). Furthermore, recent successful MARL achievements typically relied on said "Multi-Agent" versions of single-agent RL algorithms (MADDPG [15], MAPPO [34]...) which fall under a category of MARL techniques broadly referred to as "centralized training" [31]. Centralized training consists of making use of privileged global information during training to reduce the fundamental non-stationarity provoked by the evolution of others, for instance by feeding this information to a centralized critic.

In this paper, we are instead interested in studying naturally plausible evolution processes. While centralized approaches facilitate the training of deployable, high-performance policies, they of course do not qualify as such processes, nor does self-play. However, there exists a line of biologically-inspired work that is close in philosophy to self-play: "Population-Based Training" (PBT) [13]. In PBT, a population of policies is trained and periodically evaluated in a series of tournaments. These tournaments designate the "fittest" few policies to "select" and "replicate" before training continues. PBT is loosely part of a class of genetically inspired algorithms known as Evolution Strategies (ES).

The selection and replication heuristics used in ES are inspired by "imitation of the fittest", a gradient-free revision protocol through which populations of non-learning agents are thought to evolve in nature [3]. When aggregated across many agents, imitation of the fittest yields the Replicator population dynamic [24], arguably the most famous equation in Evolutionary Game Theory (EGT) [29]. Whereas MARL is often practically constrained to few-agent scenarios, EGT has long studied the evolution of large populations made of independent non-learning agents. Because these agents are non-learning, the revision protocols considered in EGT are extrinsic, similar to the genetically-inspired replicating and pruning performed in ES. However, imitation of success can also be considered as a very simple intrinsic learning protocol, where the agent simply copies the policy of its opponent based on their payoff. In this work, we bring advanced intrinsic MARL protocols to the scale of evolutionary simulations. In particular, we are interested in the evolutionary effects of Opponent-Learning Awareness, an advanced MARL protocol able to take advantage of non-stationary dynamics [10]. Our contribution is threefold:

- We show how, under common assumptions from the RL bandit literature, naive multi-agent Policy Gradient mathematically aligns with the Replicator Dynamic,
- From this result, we derive fast, parallelizable implementations of both multi-agent Policy Gradient and Opponent-Learning Awareness, targeting evolutionary simulations in pairwise matrix games,
- We perform population simulations of 200,000 learning agents and demonstrate different effects of both naive learning and Opponent-Learning Awareness on evolutionary dynamics.

This work is licenced under the Creative Commons Attribution 4.0 International (CC-BY 4.0) licence.

2 PRELIMINARIES

2.1 Evolutionary Game Theory

EGT models evolution as a series of random pairwise interactions, where interactions are typically simple bi-matrix games (i.e., 2player multi-armed bandits). Agents are sampled from a large population to be randomly paired and evaluated against their drawn opponent. The outcome of this interaction is a payoff for each opponent, whose expectation is called the agent's fitness against the current population. An agent's fitness depends on both its policy and the current configuration of the population. The agent's policy is called its *type*, which is one of *n* possible types. Agents with a greater fitness replicate and thus tend to "invade" the population, whereas agents with a lower fitness tend to go "extinct". In particular, EGT is interested in evolutionarily stable equilibria, which are configurations of the population where the different types are present in stable proportions under replication dynamics. In evolutionarily stable equilibria, the population configuration is robust to rare mutations, where few agents randomly switch from one type to another. In this paper, we will be studying more complex, learningbased types of evolutionary equilibria in three classic symmetric games: Stag Hunt, Hawk-Dove, and Rock-Paper-Scissors.

2.1.1 Stag hunt. Stag hunt (SH) is a 2-action game illustrating the evolution of cooperation. In this game, agents need to hunt for food and choose to either go for a Stag, or go for a Hare. Hunting a Hare is easy: any agent choosing this option successfully receives a payoff of 1¹. Hunting a Stag is harder: both agents need to cooperate, otherwise the agent choosing to go for a Stag fails to catch anything and receives a payoff of 0. However, if both agents cooperate, they succeed and each receives a payoff of 1.8, which is better than going for Hares. The bi-matrix representing this game is:

where rows represent the action chosen by the ego agent (bold) with corresponding payoffs in first position, and columns represent the action chosen by the other agent with corresponding payoffs in second position. The game of Stag hunt has two distinct pure strategy Nash equilibria² [20]: (1) both agents always playing Stag, and (2) both agents always playing Hare.

2.1.2 Hawk-Dove. Hawk-Dove (HD) is a 2-action game illustrating the evolution of conflict. Agents either choose to act as a "Hawk" or as a "Dove". When a Dove encounters another Dove, they share the available food (each receives a payoff of 1). When a Dove encounters a Hawk, it yields and gets no food (payoff of 0) while the Hawk gets all of it (payoff of 2). But when a Hawk encounters another Hawk, they fight and both get injured (payoff of -1 each). The bi-matrix representing this game is:

The game of Hawk-Dove has two pure strategy Nash equilibria: (1) Hawk-Dove and (2) Dove-Hawk. But note that in these equilibria, Doves have a smaller payoff than Hawks. In the context of EGT, this means that when Doves encounter almost only Hawks, they go extinct and Hawks invade. However, when Hawks encounter almost always Hawks, their payoff is even less than Doves encountering Hawks, and thus Hawks move toward extinction as Doves invade. In other words, there are population configurations in which it is not more relevant to be a Hawk than a Dove in terms of fitness, and evolutionary dynamics naturally drive the population there. Examples of such configurations are (1) a population where all agents pick Hawk or Dove uniformly at random (which is the mixed-strategy Nash equilibrium³ of this game), (2) a population formed of half deterministic Hawks and half deterministic Doves, or (3) any arbitrary population whose average behavior is to choose Hawk and Dove uniformly at random (for instance, half agents with policy $(\frac{2}{3}, \frac{1}{3})$ and half agents with policy $(\frac{1}{3}, \frac{2}{3})$...).

2.1.3 Rock-Paper-Scissors. Rock-Paper-Scissors (RPS) is a 3-action zero-sum⁴ game. It illustrates more complex situations where there are cycles in the preferences over actions. Scissors beats Paper, Paper beats Rock, and Rock beats Scissors. The bi-matrix representing this game is:

RPS has a single mixed-Nash equilibrium, where both players choose their actions uniformly at random. Similarly to the HD game, all populations whose average behavior is this equilibrium are neutrally stable under replication dynamics and drifting due to random mutations.

2.1.4 Population vector. A population whose individuals are distributed amongst n types can be represented as a population vector $P \in \mathbb{R}^n$:

$$P = \begin{pmatrix} p_1 \\ p_2 \\ \vdots \\ p_n \end{pmatrix} \text{ proportion of type 1}$$

$$(1)$$

2.1.5 Replicator Dynamic. Under the "imitation of the fittest" revision protocol (as well as several other bio-inspired revision protocols), large populations are known to follow a famous population dynamic over time (t), called the Replicator Dynamic:

$$\frac{dp_i}{dt} = p_i(v_i(P) - \bar{v}(P)) \tag{2}$$

where $v_i(P)$ is the fitness of type i in the population, and $\bar{v}(P)$ is the average fitness of all agents in the population. Denoting the vector of v_i 's as Q, the vector of all ones as 1 and the Hadamard product⁵ as \odot , Equation 2 can be written in matrix form:

$$\frac{d}{dt}P = P \odot (Q - 1\bar{v}),\tag{3}$$

¹We choose all payoff scales arbitrarily.

²2-player equilibria where each agent's best response to the other player's strategy is to always deterministically select the same action.

 $[\]overline{\,}^3$ 2-player equilibrium where both agents assign probabilities to each action.

⁴The sum of the two agents' payoffs is always 0.

⁵The matrix product takes precedence over the Hadamard product in all our notations.

2.2 Multi-Agent Reinforcement Learning

Whereas EGT typically studies evolution in the context of non-learning agents driven by extrinsic replication protocols, our work introduces intrinsic Multi-Agent Reinforcement Learning to the discussion. Instead of studying the evolutionary effects of what would be the selection heuristic of PBT, we study the evolutionary effects of what would be its learning process. Similar to EGT, we model evolution as a series of random pairwise interactions. Therefore, we are principally interested in 2-agent learning rules. In this paper, we will be specifically looking at two important such learning rules: *policy gradient* (PG), also referred to as "naive learning" in the MARL literature, and *learning with opponent-learning awareness* (LOLA) [10] in its full form (that is, using all terms in the first-order Taylor expansion, as opposed to [10]).

2.2.1 Policy gradient. Policy gradient (PG) is a fundamental learning rule from single-agent RL. It consists of following the first-order gradient of the value function with respect to the ego agent's policy parameters. Let us consider a pair of agents. We denote the ego agent as agent 1, and the other agent as agent 2. Let us further denote their respective policies as π_1 and π_2 , parameterized by vectors θ_1 and θ_2 , of current values v_1 and v_2 . The naive policy gradient is:

$$\nabla_{\theta_1} v_1(\theta_1, \theta_2) \tag{4}$$

The reason why following this gradient is considered naive in MARL is that this does not take into account the non-stationarity introduced by the learning process of agent 2.

2.2.2 Opponent-learning awareness. Learning with opponent learning awareness (LOLA) [10] is an improved version of PG that takes into account the learning process of the other agent. More precisely, LOLA models the learning process of agent 2 as if agent 2 were a naive learner and differentiates through its learning step:

$$\nabla_{\theta_1} v_1(\theta_1, \theta_2 + \Delta \theta_2) \tag{5}$$

where $\Delta\theta_2 = \eta \nabla_{\theta_2} v_2(\theta_1, \theta_2)$ is the naive learning step of agent 2, η being its learning rate. LOLA approximates this gradient by the following first-order Taylor expansion:

$$\nabla_{\theta_{1}} v_{1}(\theta_{1}, \theta_{2} + \Delta \theta_{2}) \approx \nabla_{\theta_{1}} (v_{1} + (\Delta \theta_{2})^{\top} \nabla_{\theta_{2}} v_{1})$$

$$= \underbrace{\nabla_{\theta_{1}} v_{1}}_{\text{PG}} + \underbrace{\eta (\nabla_{\theta_{1}} \nabla_{\theta_{2}} v_{1})^{\top} \nabla_{\theta_{2}} v_{2} + \eta (\nabla_{\theta_{1}} \nabla_{\theta_{2}} v_{2})^{\top} \nabla_{\theta_{2}} v_{1}}_{\text{opponent-learning awareness}}$$
(6)

Differentiating through the learning step of the opponent has two important advantages in our discussion: (1) it is a naturally plausible way of predicting the non-stationarity of the other agent (assuming agents maintain an internal model of others) in order to adapt beforehand, and (2) it enables the ego agent to adapt its own updates in order to steer the learning updates of the other agent toward its own incentives.

2.3 Population-policy equivalence

The population-policy equivalence noted by Bloembergen et al. [6] provides an interesting perspective binding evolution and Reinforcement Learning together. Let the population vector P from Equation 1 represent a population of agents playing only pure strategies, i.e., where p_i is the proportion of agents always playing

action i. Uniformly sampling agents from this population is equivalent to sampling actions from the abstract stochastic policy defined by the probability vector P. Thus, Equation 3 can be viewed as a learning process, albeit at the population level, where the evolving population of non-learning agents P is itself a self-play learning agent. In fact, Bloembergen et al. [6] show that this learning process is Cross Learning [7]. In Section 3, we show how it is possible to study large populations of learning agents with a similar analysis.

3 METHODS

To model how learning affects evolution, we adopt a philosophy similar to EGT. Namely, we consider large populations of independent learning agents, which are paired randomly at each evolution iteration and interact in normal-form matrix games. Each agent has its own learning rule (i.e., either of the two presented in Section 2.2) that it applies to its own policy after each pairwise interaction.

Whereas these rules are usually thought of in the context of persistent interactions between fixed agent pairs, in the evolutionary setting, they instead get applied after single interactions between random pairs. In other words, learning agents consider that the random opponent they interact with at each evolution step is a representative sample of the population and, for LOLA, of the current direction of its non-stationary dynamics. As hinted in Section 2.1, this yields complex population dynamics that may or may not converge to homogeneous populations, depending on factors such as the game, the learning rule, and the policy architecture.

3.1 Policy architecture

From an RL perspective, the normal-form matrix games presented in Section 2.1 are 2-agent multi-armed bandits. As this is a common assumption in multi-armed bandits [28], we consider the policy architecture parameterized by the preference vector $\theta \in \mathbb{R}^n$, where n is the number of actions, projected to the probability simplex by a simple softmax function σ , which yields the probability vector $P \in \mathbb{R}^n$ of the policy selecting each of the n available actions:

$$P = \sigma(\theta) \tag{7}$$

This policy architecture has a useful property for our derivations: its gradient has a symmetric analytical form, which is

$$\nabla_{\theta} P = (\nabla_{\theta} P)^{\top} = \operatorname{diag}(P) - PP^{\top}$$
(8)

3.2 Analytical Policy Gradient

Let us consider a symmetric normal-form game with n actions, played by a pair of agents denoted as agents 1 and 2. Since the game is symmetric, we can represent its bi-matrix as a single matrix $A \in \mathbb{R}^{n \times n}$, valid from the perspective of both agents⁶. Let us further assume that the policies of both agents are parameterized by $\theta_{1,2} \in \mathbb{R}^n$, with the simple policy architecture described in Equation 7, i.e.,

$$P_{1,2} = \sigma(\theta_{1,2}) \tag{9}$$

The value functions of both agents are:

$$v_1 = P_1^{\mathsf{T}} A P_2 \; ; \; v_2 = P_2^{\mathsf{T}} A P_1$$
 (10)

 $^{^6}A$ is formed by the first entries of the corresponding bi-matrix in Section 2.1.

Thus, the "naive" Policy Gradient of agent 1's value with respect to agent 1's parameters is:

$$\begin{split} \nabla_{\theta_1} v_1 &= \nabla_{\theta_1} P_1^\top A P_2 \\ &= (\mathrm{diag}(P_1) - P_1 P_1^\top) A P_2 \\ &= \mathrm{diag}(P_1) A P_2 - P_1 v_1 \\ &= P_1 \odot (A P_2 - v_1 \mathbf{1}) \\ &= P_1 \odot (A P_2 - \mathbf{1} P_1^\top A P_2) \\ &= P_1 \odot (Q_1 - \mathbf{1} v_1) \end{split}$$

where $Q_1 \in \mathbb{R}^n$ is the vector of action-values of the n available actions. This draws an interesting parallel with Equation 3: the PG update on the parameter vector θ_1 is the same as the Replicator update on the probability vector $P_1 = \sigma(\theta_1)$. This shows that a PG agent can itself be seen as an evolving population of abstract non-learning agents playing pure strategies, similarly to the Cross Learning equivalence noted in [6].

This formulation yields the following analytical PG formulation for symmetric normal-form games:

$$\nabla_{\theta_1} v_1 = P_1 \odot (I - \mathbf{1} P_1^\top) A P_2 \tag{11}$$

$$\nabla_{\theta_2} v_2 = P_2 \odot (I - \mathbf{1} P_2^{\mathsf{T}}) A P_1 \tag{12}$$

which only involves simple matrix operations, and therefore is a fast, easily parallelizable implementation.

3.3 **Analytical LOLA**

We now derive an analytical formulation of the LOLA update in symmetric normal-form games, similar to what we found for PG in Section 3.2. We are missing three terms from Equation 6:

- $\nabla_{\theta_2} v_1$
- $\bullet \quad \nabla_{\theta_1}^{\sigma_2} \nabla_{\theta_2} v_1 \\ \bullet \quad \nabla_{\theta_1} \nabla_{\theta_2} v_2$

To compute the first term, we note that $v_1 = P_1^{\top} A P_2$ is a scalar and thus can also be written $v_1 = P_2^{\mathsf{T}} A^{\mathsf{T}} P_1$. We can then compute this term similarly to PG:

$$\nabla_{\theta_{2}} v_{1} = \nabla_{\theta_{2}} P_{2}^{\top} A^{\top} P_{1}$$

$$= (\operatorname{diag}(P_{2}) - P_{2} P_{2}^{\top}) A^{\top} P_{1}$$

$$= P_{2} \odot (A^{\top} P_{1} - v_{1} \mathbf{1})$$

$$= P_{2} \odot (A^{\top} P_{1} - 1 P_{2}^{\top} A^{\top} P_{1})$$

$$= P_{2} \odot (I - 1 P_{2}^{\top}) A^{\top} P_{1}$$
(13)

Computing the two remaining terms is also possible. Let us start with $\nabla_{\theta_1} \nabla_{\theta_2} v_2$:

$$\nabla_{\theta_{1}} \nabla_{\theta_{2}} v_{2} = \nabla_{\theta_{1}} \nabla_{\theta_{2}} P_{2}^{\top} A P_{1}$$

$$= \nabla_{\theta_{1}} (\operatorname{diag}(P_{2}) - P_{2} P_{2}^{\top}) A P_{1}$$

$$= (\operatorname{diag}(P_{2}) - P_{2} P_{2}^{\top}) A (\operatorname{diag}(P_{1}) - P_{1} P_{1}^{\top})$$
(15)

While it would already possible to implement this formulation, we further derive a more efficient implementation in Appendix A.1:

$$\nabla_{\theta_1} \nabla_{\theta_2} v_2 = T \odot (I - \mathbf{1} P_2^\top) A (I - P_1 \mathbf{1}^\top)$$
 (16)

where $T := P_2 P_1^{\top}$.

Computing $\nabla_{\theta_1} \nabla_{\theta_2} v_1$ is fairly straightforward:

$$\nabla_{\theta_1} \nabla_{\theta_2} v_1 = \nabla_{\theta_1} \nabla_{\theta_2} P_2^{\top} A^{\top} P_1$$

$$= \nabla_{\theta_1} \nabla_{\theta_2} P_2^{\top} B P_1 \qquad (B := A^{\top})$$

$$= T \odot (I - \mathbf{1} P_2^{\top}) B (I - P_1 \mathbf{1}^{\top}) \qquad (\text{c.f. } 14,16) \qquad (17)$$

$$= T \odot (I - \mathbf{1} P_2^{\top}) A^{\top} (I - P_1 \mathbf{1}^{\top}) \qquad (18)$$

Substituting Equations 11, 12, 13, 16 and 18 in Equation 6 yields the following analytical formulation of the LOLA gradient in the symmetric normal-form game defined by matrix A:

$$\nabla_{\theta_1} v_1(\theta_1, \theta_2 + \Delta \theta_2) \approx P_1 \odot X_1 A P_2$$

$$+ \eta (T^\top \odot X_1 A X_2^\top) (P_2 \odot X_2 A P_1)$$

$$+ \eta (T^\top \odot X_1 A^\top X_2^\top) (P_2 \odot X_2 A^\top P_1) \qquad (19)$$

where $X_1 := I - \mathbf{1}P_1^{\top}$, $X_2 := I - \mathbf{1}P_2^{\top}$, and $T := P_2P_1^{\top}$.

Although the LOLA formulation of Equation 19 may look scary, it is in fact quite simple from a computational point of view. It involves only simple matrix operations, as opposed to the computationally expensive second-order gradient back-propagation normally performed by LOLA. Furthermore, batching this implementation is straightforward. These two properties make Equation 19 particularly well-suited for simulating opponent-learning awareness in large-scale evolutionary simulations.

3.4 Batched pairwise bandits

In Section 4, we demonstrate our approach by conducting verylarge-scale evolutionary simulations of heterogeneous learners, in the multi-armed bandit pairwise interactions described by the classic matrix games from Section 2.1. We study how different mixes of naive and opponent-learning aware learners affect the evolution of the population in these environments.

While Equations 11 and 19 provide very fast, backprop-free implementations of exact PG and exact LOLA in normal-form games, it would still be prohibitively slow to apply these updates iteratively on single agent pairs in evolutionary-scale simulations. EGT dynamics are usually defined for full population steps, i.e., steps in which all agents go through their revision protocol once. To make this process scalable, we batch learning updates across the entire population. More precisely, at each evolution step, we shuffle the entire population and randomly pair all agents two-by-two. Since all interactions are pairwise in evolutionary simulations, this enables batching Equations 11 and 19 across agent pairs. In fact, to optimize the process even further, we mirror all pairs to perform the entire population update in one single batched operation. This batching procedure is illustrated in Figure 1. We found batching populations in this manner to be extremely efficient. Combining this procedure with the analytical PG and LOLA implementations described in previous Sections, we are able to simulate populations of 200,000 learning agents for thousands of evolution steps in a matter of seconds on a consumer-grade GPU⁷. To ensure reproducibility and foster future work in this direction, we open-source our implementation⁸.

⁷All experiments in this paper are conducted on a Linux laptop, with an i7-12700H CPU, an RTX 3080 Ti GPU, and 64G of RAM.

⁸https://github.com/yannbouteiller/eola

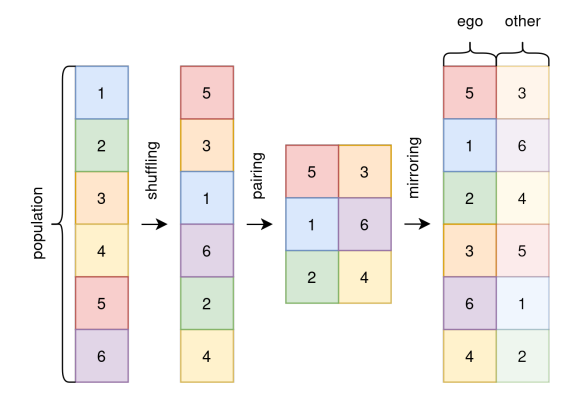


Figure 1: Pairing and batching

4 EXPERIMENTS

We demonstrate our approach by conducting large evolutionary simulations, featuring 200,000 learning agents in random pairwise interactions. We use the normal-form matrices presented in Section 2.1 as our three tested environments: *Stag hunt* (SH), *Hawk-Dove* (HD) and *Rock-Paper-Scissors* (RPS). Each individual agent has its own persistent learning rule, i.e., one of either naive learning (gradient descent with Equation 11) or opponent-learning awareness (gradient descent with Equation 19).

Because each environment exhibits different and interesting evolution dynamics for both naive and opponent-learning aware learners, we organize our results environment-by-environment. The rest of the Section is constructed as follows. First, we demonstrate the practical speed and scalability of our approach. Then, we share insights about what we expect to see happening in these experiments. Finally, we present the results of our SH, HD and RPS evolutionary learning simulations.

4.1 Scalability

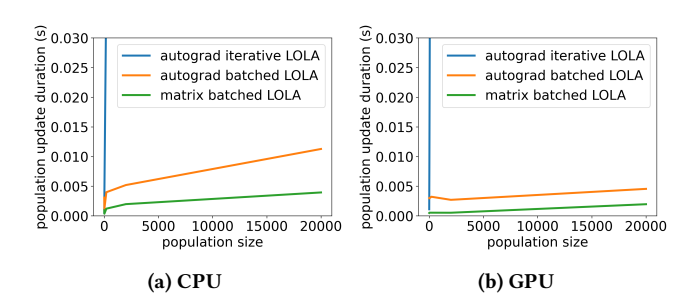


Figure 2: Timing experiments

We measure the performance of our approach across different population sizes in the RPS game. Figure 2 reports the amount of time taken to perform one LOLA update on all population members with our approach ("matrix batched LOLA"), and compares this result to two baselines. The "autograd iterative LOLA" baseline reproduces how LOLA updates are normally performed in classical multi-agent scenarios: using PyTorch's autograd to compute the

LOLA gradient, and updating the policies of all agents one after the other in an iterative fashion. This baseline is clearly not a viable implementation for evolutionary-scale simulations and is only provided for illustration. On the other hand, our "autograd batched LOLA" baseline is of more interest for future work. While the "matrix batched" approach is clearly faster, it is limited to single-shot multi-armed bandits⁹. In particular, the "matrix batched" approach does not allow using a context (state), which would be required in more complex, episodic interactions. Therefore, we have implemented the population batching approach described in Section 3.4 along with autograd, which yields a much more general implementation. We present the performance of this alternative approach as "autograd batched LOLA". Clearly, the main reason why we can perform these large-scale simulations at all is that the structure of EGT simulations enables batching policy updates. Since our matrixbased implementation is faster and works in normal-form games, we use this one in the next Sections.

4.2 Expected results

Learning, especially through advanced, non-stationarity aware rules such as LOLA, is generally avoided in EGT. MARL yields population dynamics that are difficult to predict, and, before our work, hard to simulate. Nevertheless, given the formulation of our problem, it is possible to draw some intuition of what should happen. In this paper, we are interested in very simple, single-shot bandit interactions between random pairs of learning agents. Remember how, under the population-policy equivalence described in Section 2.3, a population of pure-strategy agents can equivalently be seen as a stochastic policy over types. In our setting, agents have full stochastic policies assigning non-zero probabilities to all available actions, but are still simple stateless multi-armed bandits. Uniformly sampling a random opponent from such a population and then sampling an action from its policy is equivalent in expectation to sampling an action from the average policy of all population members. Similarly, sampling an ego agent and an action from its policy is equivalent in expectation to sampling an action from the aforementioned average policy. In other words, at least in expectation, there should be a relationship between the population dynamic, and self-play over the average policy.

4.3 Stag Hunt

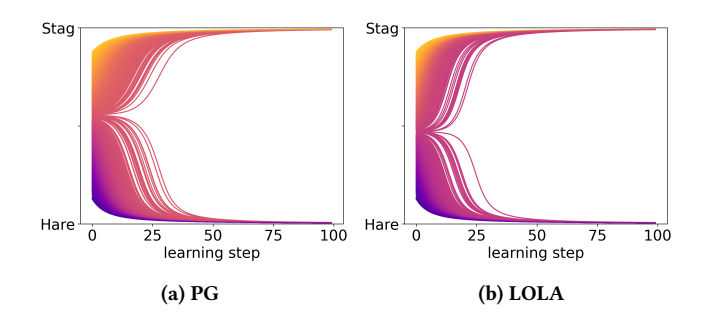


Figure 3: Self-play in Stag Hunt

 $^{^9\}mathrm{The}$ analytical implementations from Section 3 are possible mostly because the value function has a straightforward formulation in 2-agent multi-armed bandits.

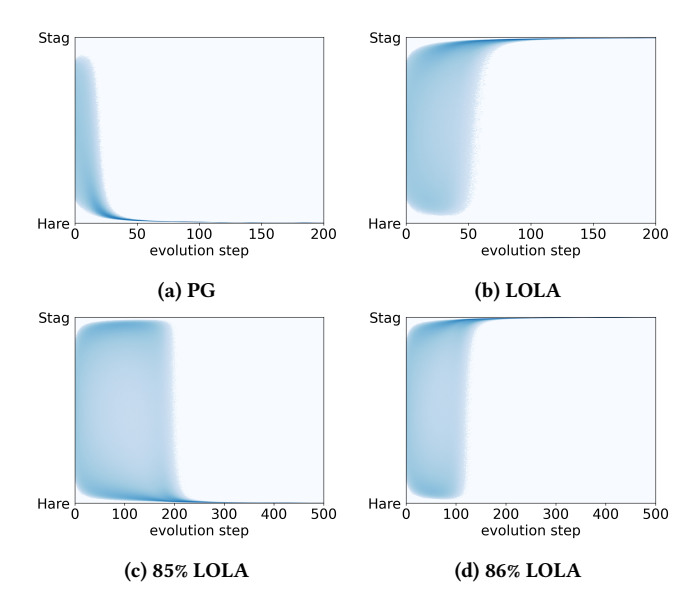


Figure 4: Evolution in Stag Hunt

Figure 3 shows how a self-play agent learns against itself in the Stag Hunt game, in a normal persistent 2-agent interaction, depending on the initial policy. The vertical axis represents the policy, with the tick in the middle being a random policy uniformly choosing between the two actions. The horizontal axis represents time expressed in learning steps. Policies are color-coded by their initial configuration, with yellow policies starting close to the deterministic Stag policy and purple policies starting close to the deterministic Hare policy. Figures 3a and 3b show how self-play behaves with naive Policy Gradient and with LOLA, respectively. Notably, Policy Gradient tends to converge to the individualistic Nash equilibrium (i.e., deterministic Hare) for most initial configurations, whereas LOLA tends to converge to the pro-social Nash equilibrium (i.e., deterministic Stag). Notice that the forks are on different sides of the uniform random policies (middle tick), which is important because we will initialize all our populations with a Gaussian distribution around this neutral policy. As explained in Section 4.2, we expect the final population dynamic to follow a pattern similar to Figure 3.

Figure 4 displays the results of our first evolutionary simulation, featuring a population of 200,000 learning agents in Stag Hunt. Dark blue areas represent high concentrations of agents, whereas lighter shades represent lower concentrations. An *evolution step* corresponds to one learning step performed per agent in the population. In Figure 4a, the population is exclusively formed of naive learners, and quickly converges to the individualistic policy, as could be expected from Figure 3a and the discussion in Section 4.2. Note however that the only reason why this argument seemingly holds is that, in our experiments, agents sample opponents from the entire population uniformly at random. In a more realistic scenario, one could decide to model locality by modifying the opponent sampling distribution, which would likely result in entirely different dynamics. In Figure 4b, the population is formed of only LOLA agents. Contrary to the naive population, a population of non-stationarity

aware learners such as LOLA evolves to unanimously adopt the superior pro-social equilibrium (i.e., deterministic Stag). Furthermore, Figures 4c and 4d report experiments where the population is made of 85% and 86% LOLA agents (the rest being naive learners), respectively. These Figures show that, when enough opponent-learning aware learners are present in the population, they become able to pull naive learners toward the pro-social strategy. In the SH game, this effect is modulated by the payoff of the pro-social strategy. We chose to present our experiments with a payoff of 1.8 because this makes the Stag strategy more difficult to reach and more interesting, but our early experiments used a payoff of 2. This initialized PG populations right around the "fork", where just 1% LOLA learners would suffice to pull the entire population instead of 86% here.

4.4 Hawk-Dove

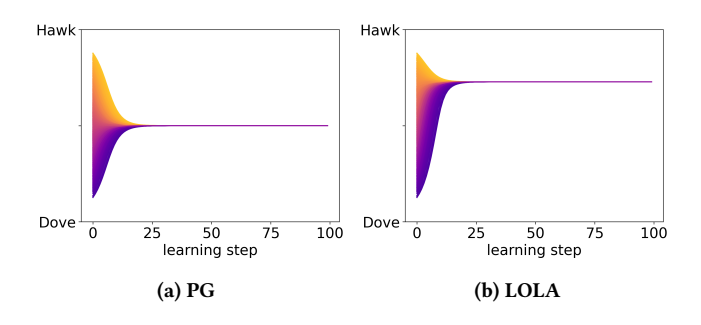


Figure 5: Self-play in Hawk-Dove

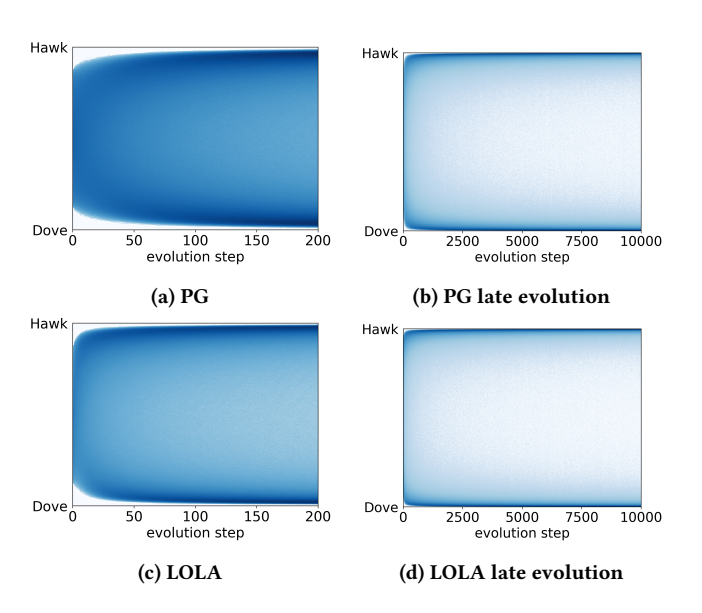


Figure 6: Evolution in Hawk-Dove

Our second experiment takes place in the Hawk-Dove game. This game is similar to the famous *Prisoner's Dilemma* but has a more interesting structure from the point of view of EGT, where it models the evolution of conflict over shareable resources [8, 26]. Contrary to SH, HD has no homogeneous pure strategy Nash equilibrium.

Instead, it has two inhomogeneous pure equilibria: Hawk/Dove and Dove/Hawk. It also has one homogeneous mixed Nash equilibrium, which is to play Hawk half of the time¹⁰. Figure 5 shows that, in this environment, self-play converges to definite policies regardless of where training starts from. Naive learning (Figure 5a) converges to the mixed Nash equilibrium, which has a payoff of 0.5 for both players. However, LOLA (Figure 5b) converges to another, inferior policy, where it selects Hawk 73% of the time (which yields a smaller payoff for both players, and is not a Nash equilibrium). A similar behavior has been described as "arrogance" in Letcher et al. [14], where both LOLA learners make wrong assumptions about the response of their opponent and thus pull away from the equilibrium. From these observations, one could imagine that all learning agents in the population would converge to these policies, similar to what we observed in Section 4.3.

But this is not at all what happens in practice. Figure 6 displays the results of our second evolutionary simulation, in the Hawk-Dove game. Whether naive learning (Figures 6a and 6b) or LOLA (Figures 6c and 6d) is used as the learning rule of the entire population, it evolves into evenly spread Hawks and Doves, most of them with close-to-deterministic policies, and in both cases with an average population policy that corresponds to the mixed Nash equilibrium (i.e., the population counts on average as many Hawks as Doves). Notice that the convergence to deterministic strategies is however much slower than what we observed in Section 4.3, and it is in fact not clear whether this will eventually happen entirely, even after 10,000 steps. Nonetheless, what can be observed from Figures 6a and 6b is that LOLA learners converge faster during early steps. Out of curiosity, we mixed LOLA and PG learners to see whether LOLA learners would be more inclined toward the Hawk strategy as hinted by Figure 5b, but we observed very similar dynamics, with the same proportion of both Hawks and Doves amongst opponent-learning aware and naive learners.

4.5 Rock-Paper-Scissors

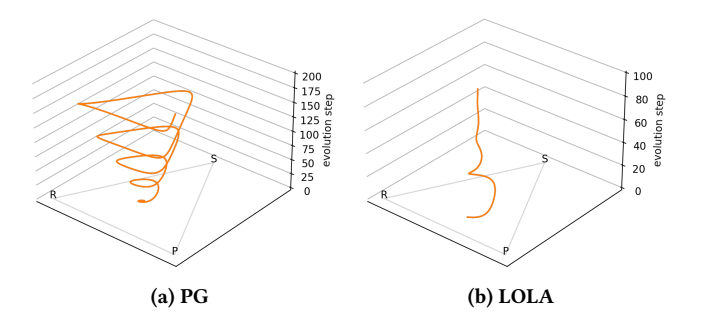


Figure 7: Self-play in Rock-Paper-Scissors

Our final population experiment takes place in the 3-action Rock-Paper-Scissors environment, used in EGT to explain the coexistence of competitively unbalanced species [1]. Interestingly, we will see that, while populations of naive learners agree with this explanation of sustainable diversity, populations of LOLA learners yield quite the opposite result. Similarly to previous Sections, figure 7 shows

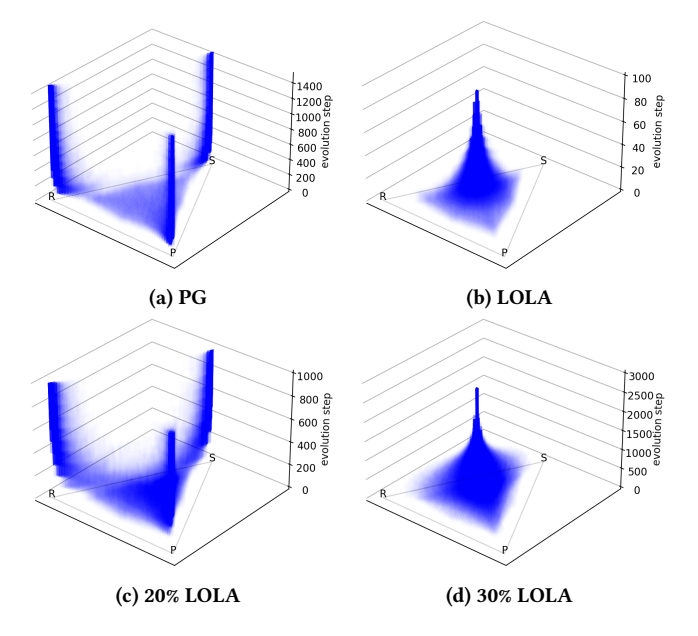


Figure 8: Evolution in Rock-Paper-Scissors

how 2-agent self-play behaves for both PG and LOLA. Only 1 policy is displayed for readability (other initial conditions yield similar effects). The triangle on the bottom of each plot represents the policy, and the vertical axis represents the number of learning steps. It can be seen that PG slowly spirals outward from the mixed Nash equilibrium (due to performing straight policy updates with a non-zero learning rate following a circular vector field), whereas LOLA quickly spirals inward until it reaches the mixed Nash equilibrium.

Figure 8 presents the results of our evolutionary simulations in the RPS game. The color-coding follows the same principle as our previous population plots, with the bottom triangle being the policy, and evolution steps being the vertical dimension. Similarly to Figure 6b, Figure 8a shows that populations of naive learners evolve into 3 equally distributed groups of close-to-deterministic agents always playing Rock, Paper and Scissors respectively. The reason why this happens is of interest, and is more clearly understood from Figure 9 in Appendix A.2. In short, this dynamic results from the loss of plasticity modeled by the softmax function¹¹. At the beginning of evolution, naive learners are erratically moving around as they encounter all types of strategies. However, after some time, agents get "trapped" near the border of the policy simplex, where gradients toward the opposite action are near-zero. After a long time, three groups of near-deterministic agents emerge, and a small number of them continuously escape toward the strategy that counters the majority group, which eventually creates a new majority, and so on, yielding a cyclic evolution pattern. In other words, diversity emerges from populations of naive learners in the RPS model. On the other hand, Figure 8b tells a different story about populations of LOLA agents, which instead quickly and unanimously converge to the mixed Nash equilibrium of this game.

 $^{^{10}\}mathrm{With}$ our choice of game matrix from Section 2.1.

 $^{^{11}\}mathrm{This}$ model is very similar to the "cost of motion" described by Mertikopoulos and Sandholm for the Replicator Dynamic [19].

4.6 Remark

From our simulation results, it looks like the mean policy averaged over the entire population always converges near a Nash equilibrium of the game, even when the learning rule itself does not converge to this equilibrium in the conventional 2-agent MARL setting (see Figures 5b and 7a). We believe that this interesting property is however merely a consequence of the uniform random opponent matching scheme that we chose to implement in this paper. For instance, let us consider an extreme opposite scheme, where all pairs would instead interact persistently. All individual pairs would then converge to the pure Nash equilibrium in the Hawk-Dove game (that is, exactly one deterministic Hawk and one deterministic Dove per pair). This would average to a uniform random policy, which only happens to coincide with the mixed Nash equilibrium in our example because of our particular choice of payoff for the Hawk/Hawk situation. Any slight modification to the cost of fighting would induce a different mixed Nash equilibrium, but would not change the pure Nash equilibrium of this game. In reality, partner selection is more structured [2] and can lead to different outcomes, which we plan to explore in the future.

5 RELATED WORK

5.1 Evolutionary Game Theory

Evolutionary Game Theory (EGT) extends classical game theory to the study of evolving populations. It originated from John Maynard Smith and George Robert Price, who laid the mathematical foundations of the field [18, 27]. Notably, Smith and Price introduced the concept of Evolutionarily Stable Strategies, formalizing how types are maintained in evolving populations. William D. Hamilton, Robert Axelrod and Richard Dawkins then famously described how cooperation arises out of self-interest in the framework of EGT [4, 8, 11]. More recently, Martin Nowak proposed five mechanisms fostering the evolution of cooperation: kin selection, direct reciprocity, indirect reciprocity, network reciprocity, and - an idea that has a long history of controversy amongst evolutionary biologists - group selection [21]. Finally, William H. Sandholm and Panayotis Mertikopoulos extended the mathematical framework available for studying EGT, by formalizing population dynamics (such as the Replicator Dynamic) under the more general class of Riemannian game dynamics [19, 24].

5.2 Opponent Shaping

Opponent shaping is a powerful technique employed in decentralized MARL to promote agent coordination and cooperation. Opponent shaping can be achieved by learning to share rewards [17, 32]. However, these methods involve learning to reward opponents when they exhibit favorable behaviors, which exacerbates the nonstationarity problem as credit assignment gets harder. Opponent-learning awareness methods such as LOLA [10], however, overcome this problem by differentiating through the learning step of the other agents. An extensive line of research recently emerged in this direction, attempting to fix diverse issues in the original LOLA formulation, such as LOLA-DiCE [9], Model-Free Opponent Shaping [16], Consistent learning with Opponent-Learning Awareness [30], and Stable Opponent Shaping [14].

5.3 Simulation

While a rich field of theory exists in the form of EGT to study evolutionary processes, few papers have focused on employing simulations to study evolution. One such paper [12] confirmed various theoretical predictions regarding cycles and their effect in games by simulating the evolution of non-learning strategies in iterated prisoner's dilemmas. Interestingly, EGT simulations have also been used by Omidshafiei et al. [22], who proposed to simulate imitation of the fittest to rank policies within a population of readily-trained agents. Finally, one work of particular interest has been conducted by Yang et al. [33], who used mean-field theory in a classical MARL scenario to reduce the environment dimensionality. In their proposed approach, naive learners approximate neighboring agents as one single, "mean-field" opponent. This essentially transforms *n*-agent MARL into pairwise MARL, thus reducing the environment complexity from the point of view of individual agents. The authors demonstrated their approach in MARL simulations featuring up to 1,000 agents. While these works simulate populations of individuals (although not close to the scale of this paper), they do not consider the inherent non-stationarity caused by other co-evolving agents.

6 CONCLUSION

We have presented a methodology enabling large-scale evolutionary simulations of independent learning agents, for both naive (Policy Gradient) and advanced non-stationarity-aware (LOLA) learning rules. We have demonstrated the scalability of our approach by performing very-large-scale evolutionary simulations of 200,000 independent learning agents, randomly interacting 2-by-2 in the classic games of Stag Hunt, Hawk-Dove and Rock-Paper-Scissors. Our work essentially explores the effect of Multi-Agent Reinforcement Learning on the usual model of evolution adopted in Evolutionary Game Theory, and demonstrates interesting dynamics originating from both naive and non-stationarity-aware learning. While the approach presented in this paper is specifically designed for normal-form matrix games (i.e., stateless 2-player multi-armed bandits), we further demonstrated the possibility of conducting similar large-scale evolutionary learning simulations in more complex, stateful environments, which we plan for future work.

REFERENCES

- Stefano Allesina and Jonathan M Levine. 2011. A competitive network theory of species diversity. Proceedings of the National Academy of Sciences 108, 14 (2011), 5638–5642.
- [2] Nicolas Anastassacos, Stephen Hailes, and Mirco Musolesi. 2020. Partner Selection for the Emergence of Cooperation in Multi-Agent Systems Using Reinforcement Learning. Proceedings of the AAAI Conference on Artificial Intelligence 34 (04 2020), 7047–7054. https://doi.org/10.1609/aaai.v34i05.6190
- [3] Jose Apesteguia, Steffen Huck, and Jörg Oechssler. 2007. Imitation—theory and experimental evidence. Journal of Economic Theory 136, 1 (2007), 217–235.
- [4] Robert Axelrod and William D Hamilton. 1981. The evolution of cooperation. science 211, 4489 (1981), 1390–1396.
- [5] Christopher Berner, Greg Brockman, Brooke Chan, Vicki Cheung, Przemysław Dębiak, Christy Dennison, David Farhi, Quirin Fischer, Shariq Hashme, Chris Hesse, et al. 2019. Dota 2 with large scale deep reinforcement learning. arXiv preprint arXiv:1912.06680 (2019).
- [6] Daan Bloembergen, Karl Tuyls, Daniel Hennes, and Michael Kaisers. 2015. Evolutionary dynamics of multi-agent learning: A survey. Journal of Artificial Intelligence Research 53 (2015), 659–697.
- [7] John G. Cross. 1973. A Stochastic Learning Model of Economic Behavior. The Quarterly Journal of Economics 87, 2 (1973), 239–266. https://EconPapers.repec. org/RePEc:oup:qjecon:v:87:y:1973:i:2:p:239-266.
- [8] Richard Dawkins. 1976. The selfish gene.

- [9] Jakob Foerster, Gregory Farquhar, Maruan Al-Shedivat, Tim Rocktäschel, Eric Xing, and Shimon Whiteson. 2018. DiCE: The Infinitely Differentiable Monte Carlo Estimator. In Proceedings of the 35th International Conference on Machine Learning (Proceedings of Machine Learning Research, Vol. 80), Jennifer Dy and Andreas Krause (Eds.). PMLR, 1529–1538. https://proceedings.mlr.press/v80/ foerster18a.html
- [10] Jakob N Foerster, Richard Y Chen, Maruan Al-Shedivat, Shimon Whiteson, Pieter Abbeel, and Igor Mordatch. 2017. Learning with opponent-learning awareness. arXiv preprint arXiv:1709.04326 (2017).
- [11] WD Hamiltron. 1964. The genetical evolution of social behavior: I. Journal of theoretical biology 7 (1964), 1–16.
- [12] The Anh Han, Flavio L Pinheiro, Simon T Powers, Julián García, and Matthijs van Veelen. 2018. No Strategy Can Win in the Repeated Prisoner's Dilemma: Linking Game Theory and Computer Simulations. Frontiers in Robotics and AI | www.frontiersin.org 1 (2018), 102. https://doi.org/10.3389/frobt.2018.00102
- [13] Max Jaderberg, Valentin Dalibard, Simon Osindero, Wojciech M Czarnecki, Jeff Donahue, Ali Razavi, Oriol Vinyals, Tim Green, Iain Dunning, Karen Simonyan, et al. 2017. Population based training of neural networks. arXiv preprint arXiv:1711.09846 (2017).
- [14] Alistair Letcher, Jakob Foerster, David Balduzzi, Tim Rocktäschel, and Shimon Whiteson. 2018. Stable opponent shaping in differentiable games. arXiv preprint arXiv:1811.08469 (2018).
- [15] Ryan Lowe, Yi Wu, Aviv Tamar, Jean Harb, Pieter Abbeel, and Igor Mordatch. 2020. Multi-Agent Actor-Critic for Mixed Cooperative-Competitive Environments. arXiv:1706.02275 [cs.LG] https://arxiv.org/abs/1706.02275
- [16] Chris Lu, Timon Willi, C. S. D. Witt, and Jakob Nicolaus Foerster. 2022. Model-Free Opponent Shaping. In *International Conference on Machine Learning*. https://api.semanticscholar.org/CorpusID:248505991
- [17] Andrei Lupu and Doina Precup. [n.d.]. Gifting in Multi-Agent Reinforcement Learning. www.ifaamas.org
- [18] J Maynard Smith. 1982. Evolution and the theory of games. Press, Cambridge (1982).
- [19] Panayotis Mertikopoulos and William H. Sandholm. 2018. Riemannian game dynamics. arXiv:1603.09173 [math.OC] https://arxiv.org/abs/1603.09173
- [20] John F Nash et al. 1950. Non-cooperative games. (1950).
- [21] Martin A Nowak. 2006. Five rules for the evolution of cooperation. science 314, 5805 (2006), 1560–1563.

- [22] Shayegan Omidshafiei, Christos Papadimitriou, Georgios Piliouras, Karl Tuyls, Mark Rowland, Jean-Baptiste Lespiau, Wojciech M Czarnecki, Marc Lanctot, Julien Perolat, and Remi Munos. [n.d.]. α-Rank: Multi-Agent evaluation by evolution. ([n. d.]). https://doi.org/10.1038/s41598-019-45619-9
- [23] Georgios Papoudakis, Filippos Christianos, Arrasy Rahman, and Stefano V. Albrecht. 2019. Dealing with Non-Stationarity in Multi-Agent Deep Reinforcement Learning. arXiv:1906.04737 [cs.LG] https://arxiv.org/abs/1906.04737
- [24] William H Sandholm. 2010. Population games and evolutionary dynamics. MIT press.
- [25] David Silver, Aja Huang, Chris J Maddison, Arthur Guez, Laurent Sifre, George Van Den Driessche, Julian Schrittwieser, Ioannis Antonoglou, Veda Panneershelvam, Marc Lanctot, et al. 2016. Mastering the game of Go with deep neural networks and tree search. *nature* 529, 7587 (2016), 484–489.
- [26] John Maynard Smith. 1982. Evolution and the Theory of Games. In Did Darwin get it right? Essays on games, sex and evolution. Springer, 202–215.
- [27] J Maynard Smith and George R Price. 1973. The logic of animal conflict. Nature 246, 5427 (1973), 15–18.
- [28] Richard S Sutton. 2018. Reinforcement learning: an introduction. A Bradford Book (2018).
- [29] Jörgen W Weibull. 1997. Evolutionary game theory. MIT press.
- [30] Timon Willi, Johannes Treutlein, Alistair Letcher, and Jakob Nicolaus Foerster. 2022. COLA: Consistent Learning with Opponent-Learning Awareness. ArXiv abs/2203.04098 (2022). https://api.semanticscholar.org/CorpusID:247315224
- [31] Annie Wong, Thomas Bäck, Anna V Kononova, and · Aske Plaat. 123. Deep multiagent reinforcement learning: challenges and directions. Artificial Intelligence Review 56 (123), 5023–5056. https://doi.org/10.1007/s10462-022-10299-x
- [32] Jiachen Yang, Ang Li, Mehrdad Farajtabar, Peter Sunehag, Edward Hughes, and Hongyuan Zha. 2020. Learning to incentivize other learning agents. In Proceedings of the 34th International Conference on Neural Information Processing Systems (Vancouver, BC, Canada) (NIPS '20). Curran Associates Inc., Red Hook, NY, USA, Article 1275. 12 pages.
- [33] Yaodong Yang, Rui Luo, Minne Li, Ming Zhou, Weinan Zhang, and Jun Wang. 2020. Mean Field Multi-Agent Reinforcement Learning. arXiv:1802.05438 [cs.MA] https://arxiv.org/abs/1802.05438
- [34] Chao Yu, Akash Velu, Eugene Vinitsky, Jiaxuan Gao, Yu Wang, Alexandre Bayen, and Yi Wu. 2022. The Surprising Effectiveness of PPO in Cooperative, Multi-Agent Games. arXiv:2103.01955 [cs.LG] https://arxiv.org/abs/2103.01955

A SUPPLEMENTARY MATERIAL

A.1 Second-order policy gradients

In this Section, we show that:

$$\nabla_{\theta_1} \nabla_{\theta_2} v_2 = T \odot (I - \mathbf{1} P_2^\top) A (I - P_1 \mathbf{1}^\top)$$

where $T := P_2 P_1^{\top}$ is agent 2's transition matrix.

Proof.

$$\nabla_{\theta_1} \nabla_{\theta_2} v_2 = \operatorname{diag}(P_2) - P_2 P_2^{\mathsf{T}} A (\operatorname{diag}(P_1) - P_1 P_1^{\mathsf{T}})$$

$$= \operatorname{diag}(P_2) A \operatorname{diag}(P_1) - \operatorname{diag}(P_2) A P_1 P_1^{\mathsf{T}} - P_2 P_2^{\mathsf{T}} A \operatorname{diag}(P_1) + P_2 P_2^{\mathsf{T}} A P_1 P_1^{\mathsf{T}}$$
(20)

Note that, for $X, Y \in \mathbb{R}^n$:

$$XY^{\mathsf{T}} = X\mathbf{1}^{\mathsf{T}} \odot \mathbf{1}Y^{\mathsf{T}}$$

since:

$$\begin{pmatrix} x_1y_1 & x_1y_2 & \dots & x_1y_n \\ x_2y_1 & x_2y_2 & \dots & x_2y_n \\ \vdots & \vdots & & \vdots \\ x_ny_1 & x_ny_2 & \dots & x_ny_n \end{pmatrix} = \begin{pmatrix} x_1 & x_1 & \dots & x_1 \\ x_2 & x_2 & \dots & x_2 \\ \vdots & \vdots & & \vdots \\ x_n & x_n & \dots & x_n \end{pmatrix} \odot \begin{pmatrix} y_1 & y_2 & \dots & y_n \\ y_1 & y_2 & \dots & y_n \\ \vdots & \vdots & & \vdots \\ y_1 & y_2 & \dots & y_n \end{pmatrix}$$

Also, for $M \in \mathbb{R}^{n,n}$ note that:

$$\operatorname{diag}(X)M = X\mathbf{1}^{\top} \odot M$$

since:

$$\begin{pmatrix} x_1m_{1,1} & x_1m_{1,2} & \dots & x_1m_{1,n} \\ x_2m_{2,1} & x_2m_{2,2} & \dots & x_2m_{2,n} \\ \vdots & \vdots & & \vdots \\ x_nm_{n,1} & x_nm_{n,2} & \dots & x_nm_{n,n} \end{pmatrix} = \begin{pmatrix} x_1 & x_1 & \dots & x_1 \\ x_2 & x_2 & \dots & x_2 \\ \vdots & \vdots & & \vdots \\ x_n & x_n & \dots & x_n \end{pmatrix} \odot \begin{pmatrix} m_{1,1} & m_{1,2} & \dots & m_{1,n} \\ m_{2,1} & m_{2,2} & \dots & m_{2,n} \\ \vdots & \vdots & & \vdots \\ m_{n,1} & m_{n,2} & \dots & m_{n,n} \end{pmatrix}$$

And similarly:

$$M\mathrm{diag}(X) = (\mathrm{diag}(X)M^\top)^\top = (X\mathbf{1}^\top \odot M^\top)^\top = M \odot \mathbf{1}X^\top$$

So, taking a closer look at each term in Equation 20:

$$\operatorname{diag}(P_2)AP_1P_1^{\top} = P_2\mathbf{1}^{\top} \odot AP_1P_1^{\top}$$

$$= P_2\mathbf{1}^{\top} \odot AP_1\mathbf{1}^{\top} \odot \mathbf{1}P_1^{\top}$$

$$= P_2\mathbf{1}^{\top} \odot \mathbf{1}P_1^{\top} \odot AP_1\mathbf{1}^{\top}$$

$$= T \odot AP_1\mathbf{1}^{\top}$$

 $\operatorname{diag}(P_2)A \operatorname{diag}(P_1) = T \odot A$

$$\begin{split} P_2 P_2^\top A & \operatorname{diag}(P_1) = P_2 P_2^\top A \odot \mathbf{1} P_1^\top \\ &= P_2 \mathbf{1}^\top \odot \mathbf{1} P_2^\top A \odot \mathbf{1} P_1^\top \\ &= P_2 \mathbf{1}^\top \odot \mathbf{1} P_1^\top \odot \mathbf{1} P_2^\top A \\ &= T \odot \mathbf{1} P_2^\top A \end{split}$$

$$P_2 P_2^\top A P_1 P_1^\top = P_2 v_2 P_1^\top = T \odot v_2 \mathbf{1} \mathbf{1}^\top$$

This enables writing the LOLA second-order gradient as:

$$\nabla_{\theta_1} \nabla_{\theta_2} v_2 = T \odot (A - AP_1 \mathbf{1}^\top - \mathbf{1} P_2^\top A + v_2 \mathbf{1} \mathbf{1}^\top)$$

The term between parentheses can be factorized:

The factorized:

$$A - AP_1 \mathbf{1}^\top - \mathbf{1}P_2^\top A + v_2 \mathbf{1}\mathbf{1}^\top = A - AP_1 \mathbf{1}^\top - \mathbf{1}P_2^\top A + \mathbf{1}v_2 \mathbf{1}^\top$$

$$= A - AP_1 \mathbf{1}^\top - \mathbf{1}P_2^\top A + \mathbf{1}P_2^\top AP_1 \mathbf{1}^\top$$

$$= (I - \mathbf{1}P_2^\top)A - (I - \mathbf{1}P_2^\top)AP_1 \mathbf{1}^\top$$

$$= (I - \mathbf{1}P_2^\top)(A - AP_1 \mathbf{1}^\top)$$

$$= (I - \mathbf{1}P_2^\top)A(I - P_1 \mathbf{1}^\top)$$

So:

$$\nabla_{\theta_1} \nabla_{\theta_2} v_2 = T \odot (I - \mathbf{1} P_2^{\top}) A (I - P_1 \mathbf{1}^{\top})$$

A.2 Rock-Paper-Scissors

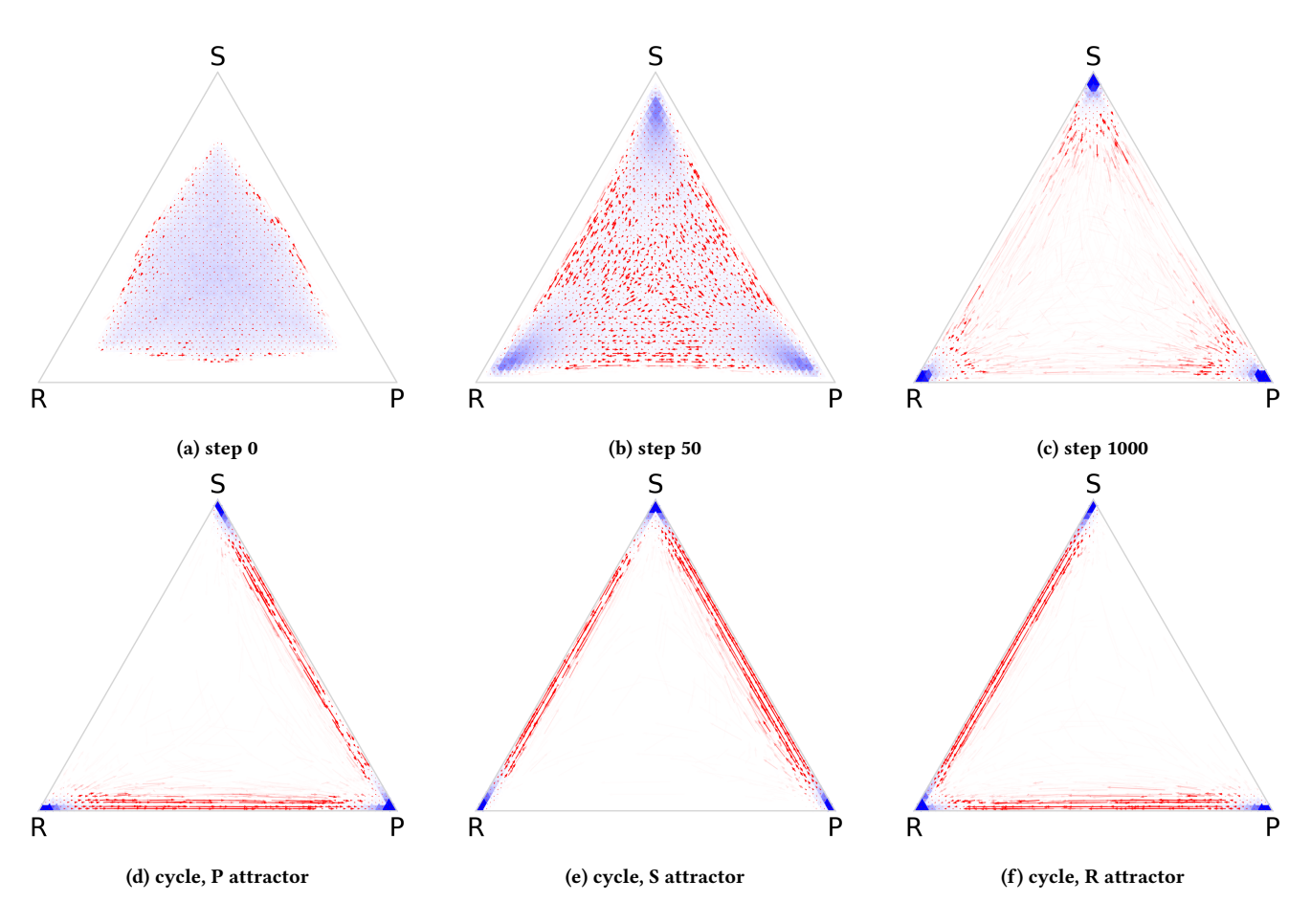


Figure 9: Naive learning in RPS, late evolution

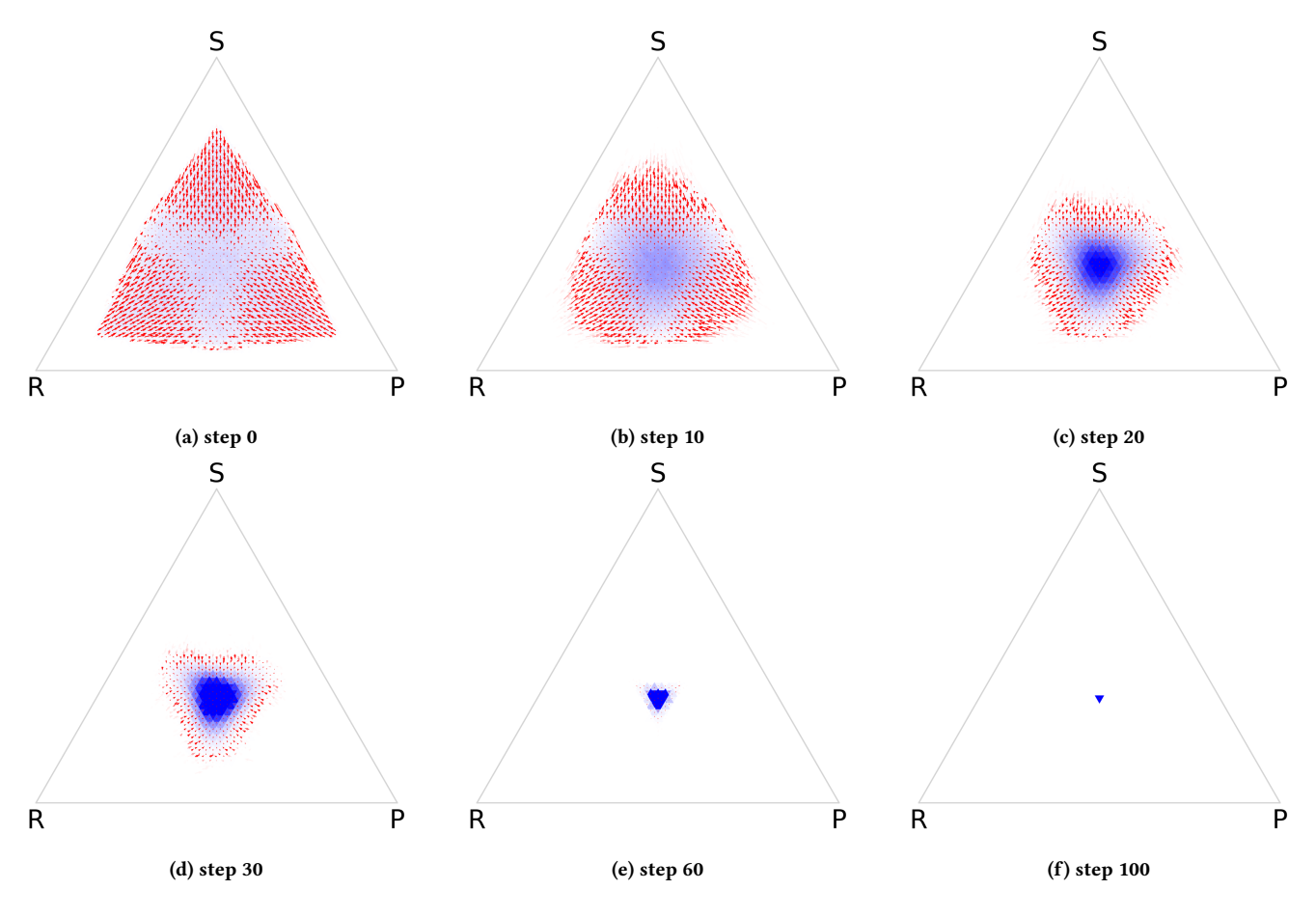


Figure 10: LOLA in RPS